TERRESTRIAL LASER SCANNER POINT CLOUD DENOISING BY RANGE IMAGE NLMEANS PROCESSING FOR SMALL-SIZED OBJECTS

E. Smigiel*, E. Alby, P. Grussenmeyer

Photogrammetry and Geomatics Group MAP-PAGE UMR 694, Graduate School of Science and Technology (INSA),
24 Boulevard de la Victoire, 67084 STRASBOURG, France
(eddie.smigiel, emmanuel.alby, pierre.grussenmeyer)@insa-strasbourg.fr

KEY WORDS: Terrestrial Laser Scanning, Denoising, Modelling, Accuracy

ABSTRACT:

In some applications, long range operations Terrestrial Laser Scanners (TLS) achieve insufficient precision: for instance, a decorated façade will not be modeled correctly with the point cloud obtained by TLS. It may be necessary, in such cases, to combine different acquisition techniques to deal with the large size of the object to model and its fine details. Hence, data denoising in the context of TLS point clouds remains an issue: if one is capable of increasing the precision of the point cloud, it makes the instrument suitable for applications it has not been designed for. The work described in this paper deals with TLS data denoising in the context of small details like in close range applications. Compared to other denoising methods described in the literature, the herein described method puts the problem back to the 2D world. Indeed, the natural product of any TLS is a Range Image, the range being a function of two angles, vertical and horizontal. In the proposed method, each acquired station is processed by denoising this 2D function. Then, after denoising, the registration process is applied to obtain the final 3D point cloud. Two well-known image denoising methods are tested: wavelet analysis and NL-means algorithm. The presented results show that the latter method achieves good results: the standard deviation is divided by two without any increase of the noise on particular points. The method which modifies slightly the standard processing chain and which inherits the algorithm complexity of the classical 2D image processing schemes allows to extend the range of applications of TLS to smaller and fine detailed objects.

1. INTRODUCTION

TLS are generally used to survey buildings or large scale objects. If one considers a façade of a building, some details are too small to be properly documented with TLS. This study aims to extend the precision of such a device. Indeed, the noise on distance measurement is typically on the order of size of several millimeters. The issue of this study is to reduce the standard deviation of the error: Rmes=Rtrue+ε, where Rmes represents the measured distance and Rtrue represents its actual value. In addition, data are distances so one has to ensure that denoising does not increase the error, even for a small number of points. The paper is organized as follows: first the general principles of a point cloud processing chain are recalled. Then, the state of the art of point cloud or mesh denoising is briefly presented. It will then be proposed an original method of denoising based on Range Image processing bringing the problem back to a conventional 2D image denoising. Among the many existing methods, the results obtained with the NLmeans algorithm will be presented compared to the wavelet denoising method. After a brief presentation of the experimental dataset, the quantitative and qualitative obtained results will be discussed.

2. THE STANDARD CHAIN: FROM ACQUISITION TO THE 3D MODEL

The standard chain from data acquisition to the final 3D model consists of different steps with many variants. Besides, each step may be realized by a wide variety of algorithms more or less automatically and is in itself a subject of research. The scope of this paragraph is to recall briefly the general idea of the standard chain which has been implemented in commercial software.

The output data of most TLS is a raw point cloud, i.e. a set of points given by at least their X, Y, Z coordinates and usually the reflected intensity of the laser pulse or sometimes more information like for instance RGB from an integrated camera. Each point cloud corresponds to one position of the laser scanner, called a station, several stations being necessary to obtain a satisfactory description of the object with a maximum amount of information.

Then, the different point clouds are registered to result in a unique point cloud for the whole object.

The next step consists in isolating the object of interest in the segmentation step.

Lastly, modeling or surface triangulation can be applied to obtain the geometrical model of the object. Further processing like texture mapping can still be applied depending on the final result one wants to obtain. Figure 1 illustrates a very basic minimum chain from data acquisition to a final model. In this model, a denoising step has been introduced in order to increase the accuracy of the point cloud.
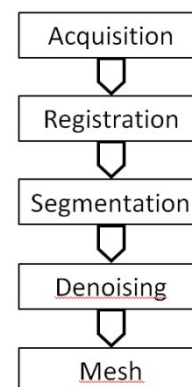

Figure 1: The standard chain from the individual point clouds to the final model.

So far, the problem of denoising has been addressed mainly through the processing of the 3D cloud or directly on the mesh. By doing so, the denoising scheme becomes independent from the acquisition step. Historically, the classical Laplacian smoothing scheme has been developed (Gross, 2000; Ohtake, 2000). To overcome the oversmoothing problem due to lowpass filtering, Wiener filtering has also been adapted successfully to 3D meshes (Peng, 2001). A second group of methods, inspired by anisotropic diffusion has also been developed (Taubin, 1995; Hildebrandt, 2004). Recently, Bilateral filtering has been introduced in the question of mesh denoising (Fleishman, 2003). Many variants and enhancements of these basic methods have been introduced, including combinations of them. Theoretical works have shown some equivalence between these methods (Barash, 2002). To conclude with this very short presentation of mesh or point cloud denoising, let us also mention recent methods based on Non Local means (Wang, 2008; Schall, 2007).

Though the care for acquisition independent methods is comprehensive, on the other hand, denoising as close as possible to the acquisition stage makes sense too for one can expect the noise to be more difficult to attenuate once cumulated in a complete 3D cloud obtained by merging of individual stations. Besides, adapting methods in the 3D case results in increased complexity, computation time and hardware resources.

The method herein proposed consists in putting back the problem into image denoising. Denoising is done within the Range Image produced by the TLS.
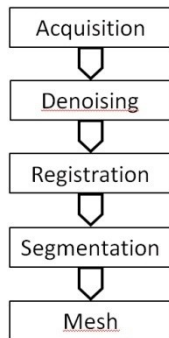

Figure 2: the proposed chain; denoising is applied before registration on the range image.

3. RANGE IMAGE DENOISING.

3.1 The image approach

In the state-of-the-art methods briefly described above, the input data is either a global point cloud or a surface mesh. The methods developed, though successful, are not standardized yet, not easy to implement and result generally speaking in great algorithm complexity. The approach that has been developed for this paper which is based on a previous work (smigiel, 2007) consists in coming back to the standard chain at the point where one does not have to deal with 3D data, i.e. on the very basic principle of laser scanning. The natural product of a TLS is the so-called Range Image $R \cdot \theta, \varphi$. If the scanning is rectangular, then this 2D function is nothing else but an image in the very classical sense with the exception that the usual intensity information (being function of two space variables) is replaced by range. Thus, spatial filtering of the point cloud may be processed as a mere image filtering with all the methods that

have been developed within the image processing community. The denoising step of standard chain exposed in figure 2 is then as shown on figure 3.
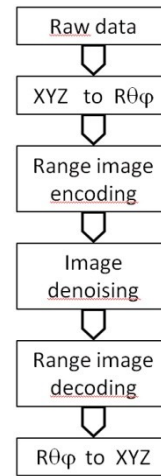

Figure 3: The denoising step included in the proposed chain of figure 2. This step is applied for each station before registration.

The raw point cloud from one station given by the (X,Y,Z) coordinates is first transformed into the (R, θ, φ) triplet (the laser scanner measures directly these values but transforms them into their X,Y,Z equivalent and outputs them in the output file). Then the (R, θ, φ) set is transformed into an image with a rectangular grid by exploiting the Δθ and Δφ information of the scan. Denoising is processed and back transformations are applied to return to a modified (X,Y,Z) description of the points set. Then, these modified (X,Y,Z) clouds may enter the standard chain described on figure 2. Hence, denoising the point cloud becomes merely a question of image denoising.

3.2 Denoising by Non local means algorithm (NL-means)

In (Smigiel et al. 2008), it has been shown that Range Image denoising by wavelets leads to interesting results but suffers from "edge effect". The overall standard deviation is reduced and the surface model looks quite denoised. However, for a small amount of points mainly distributed close to the edges of the object, noise is not well reduced if not increased. The need for a better denoising scheme exists. The NL-means algorithm has been introduced by A. Buades, B. Coll and J.M. Morel (Buades et al, 2005). It takes advantage of redundancy of natural images. In this paper, the principle of the method will be described without any mathematical proof. The reader willing to turn his attention toward the theoretical aspects may find a complete description, experimental results, discussion and a complete comparison with other classical denoising methods in (Buades et al, 2005). The herein description is directly taken from these references.

Given a discrete noisy image, $v = \{v(i)|i \in I\}$, the denoised value of pixel i is computed as a weighted average of theoretically all pixels in the image,

$$NL[v](i) = \sum_{j \in I} w(i,j)v(j)$$

Where the weights $\{w(i,j)\}_{j \in I}$ depend on the similarity between the pixels i and j with the usual conditions $0 \leq w(i,j) \leq 1$ and $\sum_{j \in I} w(i,j) = 1$.

The similarity between pixels i and j takes into account square neighborhood of fixed size centered around the two former pixels, namely N_i and N_j, and is a decreasing function of the

Gaussian weighted Euclidean distance $\|v(N_i) - v(N_j)\|_{2,a}^2$ where $a > 0$ is the standard deviation of the Gaussian kernel. Generally speaking, the weighted Euclidean distance is simply defined by

$$d_w(i,j) = \sqrt{\sum_{k=1}^{N} w_k (x_{ik} - x_{jk})^2}$$

where N is the fixed size of neighborhoods N_i and N_j, i. e. the number of components of each "vectorized pixel" $v(N_i)$ and $v(N_j)$.

In the case of the Gaussian weighted Euclidean distance, the weights w_k are a decreasing Gaussian function of the Euclidean distance from the central pixel to the surrounding one with again, the normalizing condition, $\sum_{k=1}^{N} w_k = 1$.

In the calculation of equation 1, the weights $w(i,j)$ are then defined as:

$$w(i,j) = \frac{1}{Z(i)} e^{-\frac{\|v(N_i)-v(N_j)\|_{2,a}^2}{h^2}}$$

where the normalizing factor is defined as

$Z(i) = \sum_j e^{-\frac{\|v(N_i)-v(N_j)\|_{2,a}^2}{h^2}}$ and the filtering parameter h controls the decay of the exponential function and therefore the decay of the weights as a function of the similarity between pixels i and j.
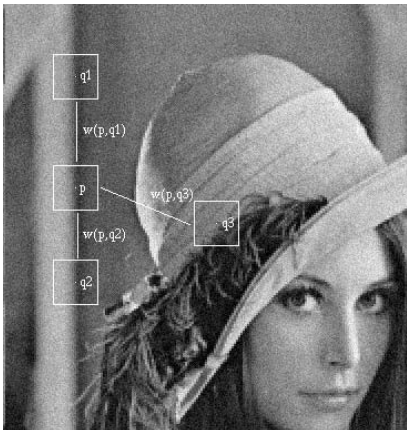

Figure 4: principle of pixels similarity in the NLmeans denoising method.

Figure 4 shows the principle of the method of the NLmeans algorithm. When calculating the value of pixel p as the weighted mean of all pixels in the image according to equation 1, pixels q_1 and q_2 are going to be associated with weights quite high as one understands intuitively that these pixels are quite similar to pixel p. On the contrary, pixel q_3 is going to weigh much less for the similarity with pixel p is quite low. Practically, the calculation of equation 1 for all pixels in the image would lead to a huge computation time. Hence, the calculation is restricted to a finite search window around the current pixel, for instance a square S x S pixels window. If the similarity window is a M x M pixels square window and if there is a total amount of N pixels in the image, the complexity of the algorithm will be $S^2 M^2 N$. According to the inventors, a similarity window of size 7 x 7 is large enough to be robust to noise and small enough to take care for details and fine structure. The size of the search window is imposed mainly by the computation time and a 21 x 21 seems to give satisfactory

results. Finally, the h parameter should be close to 10σ where σ represents the standard deviation of the noise.

4. Results

4.1 Experiments presentation

In order to test TLS data denoising (from a Trimble GX scanner), two experiments have been carried out and are presented. The NLmeans algorithm is compared to wavelet denoising on the first experiment.

The first experimental set (figure 5) consists of two Corinthian capitals of the Gallo Roman site on the modern city of Mandeure, France (2-3rd Century). Both are unfinished, which explains their morphology. Their volume is about one third of one cubic meter.
The acquisition parameters are as follows: the average distance of acquisition is between 5 and 10 m and the spatial resolution on the object is between 2 and 4 mm. Each point is measured by averaging 4 laser shots. Three stations have been completed. The total amount of points in the registered point clouds is around 350000 per capital.
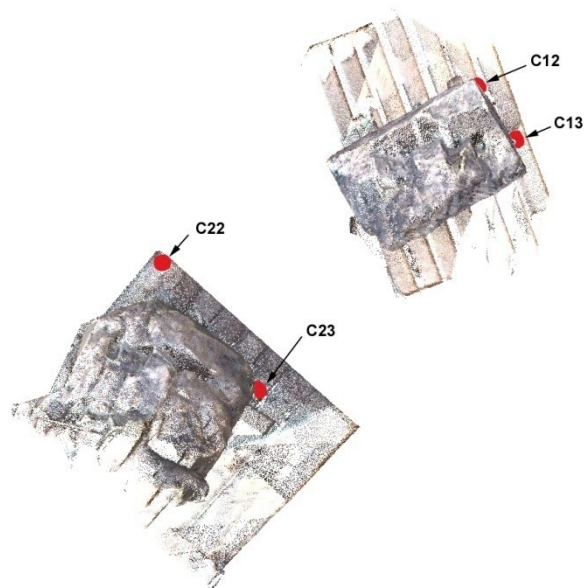

Figure 5: overview of the two capitals and the four spheres.

The second experiment is about a fragment of a Corinthian capital (figure 6) corresponding to an element of decoration. Its volume is about 4 cubic decimeters. The acquisition parameters for this fragment are as follows: the average distance of acquisition is between 8 and 9 m and the spatial resolution on the object is between 1 and 2 mm. Each point is measured by averaging 4 laser shots. Only one station has been completed. The amount of points for the fragment is around 30000.

Because of their sizes, these objects are outside the range of dimensions recommended by the TLS manufacturer, particularly for the fragment. This latter has also been acquired with a scanning arm with an accuracy of one tenth of a millimeter. It will be considered as a reference cloud. It may therefore be possible to make a full quantitative control over an object of arbitrary geometry. The comparison has been made with a point cloud from a single station.
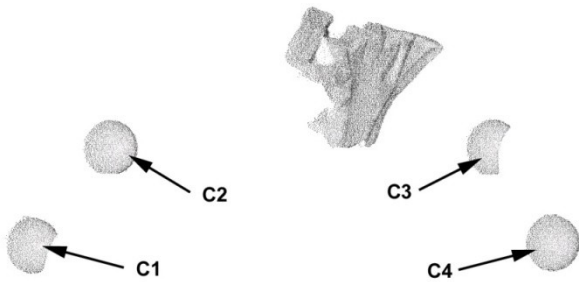
Figure 6: overview of the fragment of capital and the four spheres.

Registration calibrated spheres were regularly distributed in the environment of the object in both cases. They may be subject to a quantitative control which consists of modeling a mathematical sphere on the corresponding part of the point cloud then determining the standard deviation of the cloud from the spherical geometry.

The process applied to the point cloud ends with a mesh. The resulting mesh makes possible the visual comparison with the real object. Noise is apparent by the abrupt changes of orientation of facets particularly on smooth surfaces. It is relevant that the mesh after denoising is not smoothed at sharp edges.

	sphere name	average standard deviation (mm)	standard deviation (mm)	standard deviation (mm)	standard deviation (mm)
Raw Data			Station1	Station2	Station3
	C12	2.50	2.69	1.57	3.25
	C13	2.19	2.03	1.78	2.76
	C22	1.59	1.99	1.37	1.41
	C23	1.91	1.91	1.85	1.96
Wavelet Data					
	C12	2.23	1.45	3.61	1.62
	C13	1.99	1.78	2.39	1.81
	C22	3.23	2.57	4.06	3.06
	C23	1.94	2	2.15	1.68
Nlmeans data					
	C12	0.86	0.69	1.12	0.78
	C13	1.03	0.76	1.54	0.8
	C22	1.11	1.21	0.95	1.17
	C23	0.95	0.7	1.25	0.89

Table 1: Standard deviation on registration spheres for Capitals.

Table 1 shows the standard deviation of the points around the mathematical spheres for the two capitals of the first experiment. The average standard deviations obtained after wavelet denoising cannot emphasize a clear trend. Indeed, the standard deviations on spheres C12 and C13 are slightly improved while C23 remains almost unchanged and C22 becomes even worse. However, the average standard deviations obtained after NLmeans denoising are relatively homogeneous and lead to an average improvement by a factor of two, on the average of the four spheres. Concerning the data of the fragment, only two types are compared here, raw data and NLmeans denoised data. The results shown in table 2 confirm the previous trend: relatively homogeneous reduction of the standard deviation of a factor two on average.

	spheres	standard deviation (mm)
Raw Data		
	C1	1.91
	C2	2.04
	C3	1.86
	C4	1.86
Nlmeans data		
	C1	0.83
	C2	0.67
	C3	1.07
	C4	0.72

Table 2: Standard deviation on registration spheres for the fragment.

S1C12	X (mm)	Y (mm)	Z (mm)
Raw	-344.2	-3306.05	-1127.31
Wavelet	-343.98	-3306.02	-1128.04
Nlmeans	-343.94	-3306.35	-1127.69
S1C22			
Raw	-1712.71	-4228.28	-1137.3
Wavelet	-1712.23	-4228.55	-1136.96
Nlmeans	-1712.39	-4228.43	-1137.58

Table 3: position of the sphere in raw data and denoised data

The verification on the position of the spheres after denoising was carried out. Table 3 shows that they have not moved between the raw data and denoised ones nor for wavelet denoising neither for NLmeans algorithm. It is indeed important in the context of registration that spheres remain as rigorously as possible in their original position.

To compare several point clouds obtained in different conditions, the reference cloud has been downsampled to reach a density five times greater than for the GX data. Moreover, this cloud has been meshed to calculate the distance of each point to the reference. The error distributions of clouds (respectively the raw cloud and the denoised one) compared to the reference surface are shown on figure 7. It can be seen that the distribution is almost Gaussian (with a slight asymmetry though) and that the standard deviation of error values of the denoised cloud is twice smaller than for raw data.
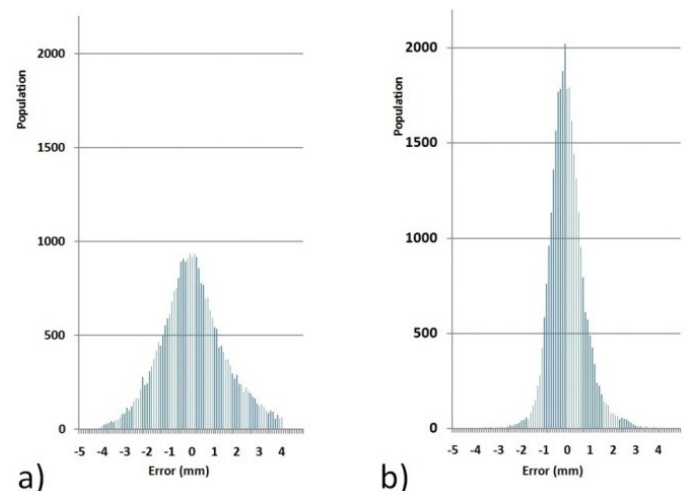

Figure 7: error distribution of points compared to the reference surface for a) raw data and b) denoised data by NLmeans.

The analysis of denoised data ends with a qualitative comparison in both experiments. Figure 8 shows the results for the first experiment and figure 9, the results for the second experiment. Concerning figure 8 and compared to the mesh

obtained from raw data, mesh calculated on denoised clouds both with wavelet and NLmeans show an improvement of the shape: the smooth surfaces of the real object do not exhibit sudden changes of the orientations of their facets no more. The edges are well preserved especially for the hole close to the bottom of the capital. However there is a difference between the two meshes: the one resulting from wavelet denoising shows an edge effect, in the sense that the edges of the processed area are badly denoised even degraded compared to the raw cloud. Although it represents only a minority of points in the cloud affecting the standard deviation not too much, the metric point of view of this study makes wavelet denoising practically useless. This weakness is not noticeable on the denoised cloud by NLmeans, which seems therefore to be a suitable method.
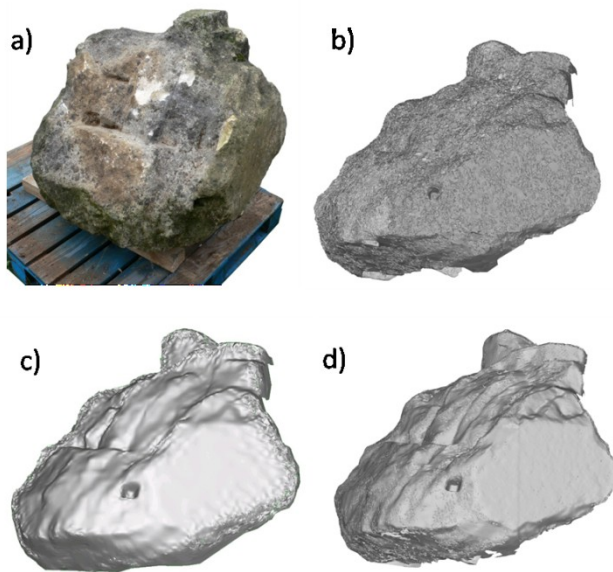

Figure 8: a) picture of one of the two Corinthian capitals, meshes obtained on b) raw data, c) wavelet denoised data and d) NLmeans denoised data.

Concerning the fragment, the mesh has been obtained from one unique station which implies a lack of data on the edges of the object. Hence, the quality of the mesh is poor on the edges not because of the denoising scheme but because of this lack of data. Though some fine details appearing on the reference have disappeared on the mesh obtained from the denoised cloud, the comparison between the raw data and the denoised data shows a clear improvement. Anyhow, the size of this object which can be considered as clearly outside the range of theTLS, makes it an extreme situation
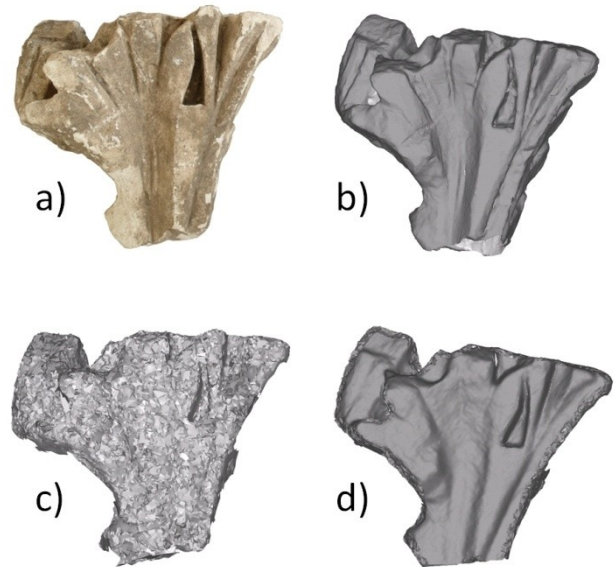

Figure 9: a) picture of the capital fragment, meshes obtained on b) the reference cloud , c) raw data and d) Nlmeans denoised data.

5. Conclusion

In this study, an original method for TLS data denoising has been proposed. It fits into the standard chain of TLS data processing, and changes it slightly. It brings the problem back to a classical 2D image processing task, which reduces the complexity of the implemented algorithms. The processed image is a range image, which implies a greater requirement on the statistics of the denoised data. One has to make sure that the error is not only improved as regard to its standard deviation but also on each individual point contrary to a classic intensity image. Hence, the mere control of the signal to noise ratio is not sufficient. Two methods of image denoising have been tested. The first one uses wavelet analysis. It improves the standard deviation in some zones and leads to a mesh of better quality than the raw data. Nevertheless, the troubles of edge effects are prohibitive for our specific application. Furthermore the management of the many parameters associated with its principle leads to heavy manipulation. The second method replaces the latter and appears in both points of view more effective. Indeed, based on NLmeans, it allows a decrease of the standard deviations of a factor of two without local deterioration (edge effects). Furthermore, the implementation of the algorithm requires only the setting of three parameters. The method enables to extend the range of application of TLS to small dimensions objects.

REFERENCES

References from Journals:

Fleishman, S., Drori, I., Cohen-Or, D., 2003. Bilateral Mesh Denoising. *ACM Trans Graphics*, vol. 22, pp. 950-953.

Barash, D., 2002. A fundamental relationship between bilateral filtering, adaptive smoothing and the nonlinear diffusion equation. *IEEE Trans. Pattern Analysis and Machine Intelligence*, vol. 24, no. 6.

Buades, A., Coll, B. & Morel, J., 2005. A Review of Image Denoising Algorithms, with a New One. Multiscale Modeling & Simulation, 4(2), 530, 490.

Buades, A., Coll, B. & Morel, J., 2005. A non-local algorithm for image denoising. Dans Computer Vision and Pattern Recognition, 2005. CVPR 2005. IEEE Computer Society Conference on. pp. 60-65 vol. 2.

Schall, O., Belyaev, A. & Seidel, H., 2007. Feature-preserving non-local denoising of static and time-varying range data. Dans Proceedings of the 2007 ACM symposium on Solid and physical modeling. Beijing, China: ACM, pp. 217-222.

Wang, R. et coll., 2008. Similarity-based denoising of point-sampled surfaces. Journal of Zhejiang University - Science A, 9(6), 807-815.

References from Other Literature:

Gross, M., Hubeli, A, 2000. Fairing of nonmanifolds for visualization. Proceedings of IEEE Visualization, 407-414.

Ohtake, Y., Belyaev, A. and Bogaeski, I, 2000. Polyhedral surface smoothing with simultaneous mesh regularization. Proceedings of Geometric Modeling and Processing, 229-237.

Peng, J., Strela, V., Zorin, D., 2001. A simple algorithm for surface denoising. Proceedings of IEEE Visualization, pp. 107-112.

Taubin, G., 1995. A Signal Processing Approach for Fair Surface Design. SIGGRAPH '95 Conf. Proc., pp. 351- 358.

Hildebrandt, K., Polthier, K., 2004. Anisotropic Filtering of Non-Linear Surface Features. Eurographics '04, vol. 23, no. 3.

Smigiel, E., Callegaro, C., Grussenmeyer, P., 2007. Digitization of the collection of moldings of the university Marc Bloch in Strasbourg: a study case. XXI International CIPA Symposium, 2007.

Smigiel, E., Alby, E., Grussenmeyer, P. (2008). Terrestrial Laser Scanner Data Denoising by Range Image Processing for Small-Sized Objects.
In: XXIth ISPRS Congress, Beijing, China, 3-11 July 2008, Int. Archives of Photogrammetry, Remote Sensing and Spatial Information Sciences,
Comm. V, ISSN 1682-1750, Vol. XXXVII, part B5, pp. 445-450.